PCCP

Adsorption of Acrolein and its Hydrogenation Products on Cu(111)

Journal:	*Physical Chemistry Chemical Physics*
Manuscript ID	CP-ART-08-2022-003817.R1
Article Type:	Paper
Date Submitted by the Author:	21-Sep-2022
Complete List of Authors:	Islam, Arephin; University of Illinois Chicago, Chemistry Molina, David ; University of Illinois Chicago, Chemistry Trenary, Michael; University of Illinois Chicago, Chemistry

ARTICLE

Adsorption of Acrolein and its Hydrogenation Products on Cu(111)

Arephin Islam, David L. Molina, and Michael Trenary *

Received 00th January 20xx,
Accepted 00th January 20xx

DOI: 10.1039/x0xx00000x

The adsorption of acrolein and its hydrogenation products propanal, 1-propanol, and 2-propenol on Cu(111) was studied by reflection absorption infrared spectroscopy (RAIRS) and temperature-programmed desorption (TPD). The experimental RAIR spectra were obtained by adsorbing multilayers of each molecule at 85 K and then annealing the surface up to 200 K to desorb the multilayer and produce the most stable monolayer structure on the surface. Each of the four molecules adsorbs weakly to the surface and desorbs at temperatures below 225 K. Compared to acrolein and propanal, the two alcohols, 2-propenol and 1-propanol, have notably higher desorption temperatures and broadened and redshifted O-H stretches that reveal strong hydrogen bonding in the multilayers. Upon annealing to 160 K, the OH stretches of both 2-propenol and 1-propanol disappear, indicating the hydrogen bonding in the multilayers is not present in the monolayers. For 2-propenol, the hydrogen bonding in the multilayer correlates with the observation of the C=C stretch at 1647 cm^{-1}, which is invisible for the monolayer. This suggests that the C=C bond is parallel to the surface for monolayer coverages of 2-propenol. Similarly, for propanal, the C=O stretch peak at 1735 cm^{-1} compared to those at 1671 and 1695 cm^{-1} is very weak at low coverages but becomes the most prominent peak for the multilayer, indicating a change in molecular orientation. For acrolein, the out-of-plane bending modes are more intense than the C=O stretch at submonolayer coverages, indicating that the molecular plane is mainly parallel to the surface. In contrast, the opposite intensity trend was observed for multilayer acrolein, suggesting that the C=O bonds are tilted away from the surface.

1. Introduction

There is considerable interest in the use of catalysts to selectively hydrogenate α,β-unsaturated aldehydes to form the corresponding unsaturated alcohols.[1] Unsaturated alcohols are used in the production of pharmaceuticals, perfumes, flavourings, thermoplastic copolymers with styrene, and acrylates in coatings, printing inks, toners, and as a source of hydroxyl functionality for crosslinking and as a resin modifier.[2-4] Acrolein (C_3H_4O) is the simplest α,β-unsaturated aldehyde and has three possible hydrogenation products: propanal, 2-propenol, and 1-propanol. The absence of substituents on the C=C group to destabilize the interaction with the catalyst surface makes it difficult to selectively hydrogenate acrolein to the desired product, 2-propenol.[5-7] Generally, it has been established that thermodynamics favours hydrogenation at the C=C bond to form the saturated aldehyde propanal. Therefore, kinetic manipulation is required for hydrogenating at the C=O bond to form 2-propenol.[7]

A new class of catalyst known as single-atom-alloys (SAAs) shows great promise for selective hydrogenation reactions.[8] SAAs consist of catalytically active dopant metal atoms substituted into the topmost atomic layer of a relatively inert host metal. High selectivity can often be achieved with the host metal at the expense of reactivity, whereas high reactivity can be achieved with the dopant metal at the expense of selectivity. In a recent study, we have reported selective hydrogenation of acrolein on the Ag(111), and Pd/Ag(111) SAA surfaces.[9] Because H_2 does not dissociate on Ag(111) and H atoms don't spill over from Pd to Ag sites on the Pd/Ag(111) SAA,[9, 10] the hydrogenation reactions were studied by exposure to atomic hydrogen. Under the most favourable conditions, a 19% selectivity was found for the partial hydrogenation of acrolein to 2-propenol, while a maximum selectivity to propanal was 91%. Unlike the Pd/Ag(111) SAA, on a Pd/Cu(111) SAA, H atoms spill over to Cu sites following H_2 dissociation on the isolated Pd atoms.[11, 12] Therefore, the Pd/Cu(111) SAA provides a promising surface for achieving selective hydrogenation of acrolein using H_2 rather than atomic H as the hydrogen source. To better understand the hydrogenation pathways of acrolein over a Pd/Cu(111) SAA, it is important to first obtain a comprehensive set of data for the interaction of acrolein and its three hydrogenation products with the Cu(111) surface.

[a] Department of Chemistry, University of Illinois Chicago, 845 W. Taylor St. Chicago, Illinois 60607, USA E-mail: mtrenary@uic.edu

Several relevant prior studies exist, although a comparative study of all four molecules adsorbed on Cu(111) is not available in the literature. Low-temperature RAIR spectra have been obtained for acrolein, 2-propenol, and propanal on Pd(111).[13] Using vibrational spectroscopy, acrolein has been studied on various surfaces, such as Au(111)[14], Pt(111)[15], Ru(001)[16], Ni(111)[15], Ag(111)[14], and a Ag thin film.[17] The adsorption geometry can be inferred by analysing the intensity of the out-of-plane modes (formyl (CH_f) and vinyl (CH_v) bends, and $=CH_2$ wag) relative to that of the C=O stretch. Compared to the C=O stretch, the out-of-plane modes are much more intense on less reactive metals such as Au(111) and Ag(111), implying a parallel adsorption geometry. The opposite is observed on the more reactive metals, indicating tilting at the C=O groups, with the tilt increasing with increasing exposure. We have previously shown that all possible hydrogenation products can be produced during the hydrogenation of acrolein on Ru(001).[16] For a Pt/Ru(001) surface, the desorption yields are minimal as most of the acrolein either desorbs molecularly or eventually decomposes to CO and H_2.[18] Dostert et al.[19] showed in a combined pulsed molecular beam and in-situ RAIRS study of acrolein hydrogenation on Pd(111) under isothermal conditions that the formation of 2-propenol with nearly 100% selectivity was possible. In studies similar to the present one, adsorbed 1-propanol has been studied on Cu(111)[20], and 1-propanol and propanal have been studied on Rh(111).[21] The desorption of propanal formed from the oxidation of propylamine on an oxygen-covered Au(111) surface has also been reported.[22] Here, we focus on comparing results obtained on Cu(111) with our recent study of these four molecules on Ag(111).[23]

2. Experimental

The experiments were performed in two separate ultrahigh vacuum (UHV) chambers. The RAIRS experiments were done in a dual- stainless-steel chamber ultrahigh vacuum (UHV) system described elsewhere[24]. Briefly, the upper UHV analysis chamber was equipped with PHI 15-120 low energy electron diffraction (LEED) optics, PHI 10-155 cylindrical mirror analyser for Auger electron spectroscopy (AES), a Hiden HAL201/3F quadrupole mass spectrometer for temperature-programmed desorption (TPD), and an ion gun for sample cleaning with Ar^+ sputtering. The inner surface of the lower chamber was coated with gold via physical vapor deposition from a resistively heated evaporator. It is equipped with two high-precision leak valves with separate gas lines and a cold cathode gauge for pressure measurements from UHV to 1500 Torr. The detailed design of the high-pressure IR cell and the evaporator will be published elsewhere. All gas exposures herein were performed in this well-baked high-pressure IR cell. The inert gold-coated walls reduced the adsorption of potential contaminants that could be subsequently deposited onto the crystal surface. During the RAIRS experiments, the main chamber was isolated from the IR cell so that the pressure in the latter could be increased up to atmospheric pressure from its base pressure of 1.0×10^{-9} Torr, while an ion pump maintained the base pressure in the main chamber. The RAIRS measurements were performed with a Bruker Vertex 70v FTIR spectrometer with an external MCT detector using 1024 scans and a resolution of 4 cm^{-1} (acquisition time of 4 minutes per spectrum). The TPD analyses at low exposures were done in a chamber with a base pressure of 1×10^{-10} Torr. All TPD results presented here were obtained with a linear heating rate of 0.5 K/s.

The Cu(111) crystal (99.9999%) was purchased from the Surface Preparation Laboratory, and its mounting in the chamber has been described elsewhere.[25] The surface was cleaned by Ar^+ sputtering at room temperature for 60 min (Ar pressure, 5×10^{-5} Torr; energy, 1.5 KeV; ion current, 9 μA) followed by annealing via resistive heating at 950 K for 10 min. After 2 to 3 cycles of sputtering and annealing, the crystal was cooled down to room temperature, and the surface cleanness was verified by AES and RAIRS of adsorbed CO. A 1×1 LEED pattern was obtained after the crystal had been cleaned. A constant current power supply (B&K Precision, 1900B series) controlled with a PID controller (Eurotherm 2416) provided direct heating to the Cu(111) crystal and maintained the temperature within 0.1 K.

1-propanol (≥99.5%, Sigma Aldrich), 2-propenol (≥99%, Sigma Aldrich), and propanal (≥99%, Acros Organics) were purified by multiple freeze-pump-thaw cycles with a liquid nitrogen bath. Acrolein (Alfa Aesar, 96%, stabilized with hydroquinone) was purified to eliminate possible decomposition products such as ethylene by successive freeze-pump-thaw cycles with liquid nitrogen followed by a methanol/liquid nitrogen mixture cold bath.

3. Results and Discussion

Acrolein and its hydrogenation products 2-propenol, propanal, and 1-propanol were adsorbed on the Cu(111) surface and studied as a function of exposure in Langmuir units (1 L = 1×10^{-6} Torr sec) with RAIRS and TPD. To understand adsorption geometries and to determine if any reaction products formed upon heating, the surface was dosed with the corresponding gases at 85 K, then annealed to a given temperature, held there for one minute, and cooled back to 85 K where the spectra were acquired. In addition, TPD spectra were collected following exposures to the Cu(111) surface at 85 K. Each of the four gases studied here produces very similar mass fragments, which makes definitive identification of the desorbing species difficult. For this study, the fragmentation ratios for each of the pure compounds were collected. Then the best mass fragments were selected for monitoring the desorption of a particular compound.

3.1 Acrolein

Fig. 1a shows RAIR spectra versus acrolein exposure on Cu(111) at 85 K. At low exposures (below 1.5 L), the IR bands seen at 923 and 991 cm^{-1} correspond to the in-plane CH_2 rocking mode ($\rho(CH_2)$) and out-of-plane wag ($\omega(CH_2)$) mode and at 1181 cm^{-1} to the C-C stretch. With increasing exposure, these peaks redshift and increase in intensity while a new peak at 1165 cm^{-1} appears and becomes prominent at high exposure. In addition, for low exposures, the C=O stretch is observed at 1699 cm^{-1}, slightly lower than its gas phase value of 1724 cm^{-1}. The peak intensity of the C=O stretch increases with increasing exposure and gives rise to a secondary peak at 1651 cm^{-1}. In addition to the C=C stretch peak at 1617 cm^{-1}, the secondary peak, due to the interactions of the C=O bond with neighbouring acrolein molecules, indicates multilayer formation. The very weak peaks at 1366 and 1426 cm^{-1}, assigned to formyl CH and the CH_2 bending modes, respectively, become strong at high exposures. At high exposures and for multilayers, the C-H stretch region shows four features. The peaks at 2769 and 2709 cm^{-1} correspond to the first overtone of the vinyl CH bend and the formyl CH stretch, while the peaks at 2822 and 2855 cm^{-1} correspond to the CH_2 symmetric and antisymmetric stretches, respectively. The features at about 1114 and 1539 cm^{-1} remain unchanged for all exposures and are unassigned.

The calculated vibrational frequencies for *trans*- and *cis*-acrolein were compared to the experimental gas phase and Ar matrix IR spectra by Puzzarini et al.[26] In the gas phase, the C-C stretch is at 1056 cm^{-1} for *cis*-acrolein and at 1158 cm^{-1} for *trans*-acrolein. Here, we do not observe any features indicating *cis*-acrolein on Cu(111), and previous studies have shown that *trans*-acrolein is the most stable form on Ag surfaces.[14, 23] Table 1 presents the assignments of the peaks seen here to the vibrational modes of *trans*-acrolein and a comparison to the peak positions previously reported for adsorbed acrolein.

Fig. 1b shows RAIR spectra (in red) after 4.0 L of acrolein was adsorbed on the Cu(111) surface at 85 K and then annealed to the indicated temperatures. Annealing allows more stable adsorption structures to develop by overcoming kinetic barriers that trap less stable structures formed upon adsorption at 85 K. TPD results versus acrolein exposure are shown in Fig. 2. Other results (not reported here) have shown that at even higher exposures, a third peak develops at 115 K for a 5 L exposure and is attributed to multilayer desorption whereas the 138 K peak corresponds to 2^{nd} layer acrolein molecules. The peak in the range of 225-219 K corresponds to desorption of the monolayer. After annealing at 130 K, big changes are seen in Fig. 1b in the relative intensities of the peaks; before annealing the C=O stretch at 1699 cm^{-1} is most intense, whereas after the annealing the CH_2 wag at 991 cm^{-1} is most intense. Other notable changes include the disappearance of the in-plane CH_2 rock at 923 cm^{-1}. Comparison with Fig. 2 indicates that annealing to 130 K should desorb the multilayer leaving 2^{nd} layer and monolayer acrolein on the surface. The TPD results also imply that annealing to 145 and 160 K should desorb the 2^{nd} layer to leave monolayer acrolein on the surface. The changes in the spectra upon annealing to 130 K with the out of plane modes giving the most intense peaks suggest that 2^{nd} layer acrolein molecules are oriented with the molecular plane parallel to the surface, whereas in the multilayer at least some of the molecules are oriented with the molecular plane tilted with respect to the surface. As noted by Itoh and co-workers, the initial greater intensities of the out-of-plane CH_x wags over the C=O stretch imply a parallel bonding geometry for acrolein on Au(111) and Ag surfaces.[14, 17] Our results imply that while the 2^{nd} layer molecules have detectable out-of-plane modes. For monolayer molecules, which are presumed also to be oriented parallel to the surface, even these out-of-plane modes are too weak to detect.

The parallel bonding geometry of the planar molecule implies that acrolein interacts with Cu(111) through π-bonding at the C=O and C=C double bonds. Although the interaction of acrolein with Cu(111) and Ag(111) is similar, there are notable differences. On Ag(111) the monolayer TPD peak occurs at 164 K at the lowest coverage and shifts to 170 K at the highest coverage, indicating that adsorbate-adsorbate interactions stabilize acrolein adsorption. On Cu(111), the monolayer TPD peak starts at 225 K and decreases to 219 K as the coverage increases, indicating that adsorbate-adsorbate interactions are slightly destabilizing. The higher temperatures at which monolayer acrolein desorbs compared to Ag(111) indicates a stronger interaction with Cu(111). This is also reflected in differences in the RAIRS results for the two surfaces. Once the multilayer is desorbed from both surfaces, the most intense peaks are due to out of plane bending modes. However, at low monolayer coverages the C=O stretch occurs at 1676 cm^{-1} on Ag(111), which is shifted from its gas phase value of 1724 cm^{-1}. Attributing the 1699 cm^{-1} peak to the C=O stretch of 2^{nd} layer acrolein on Cu(111) is consistent with only an indirect interaction with the metal surface.

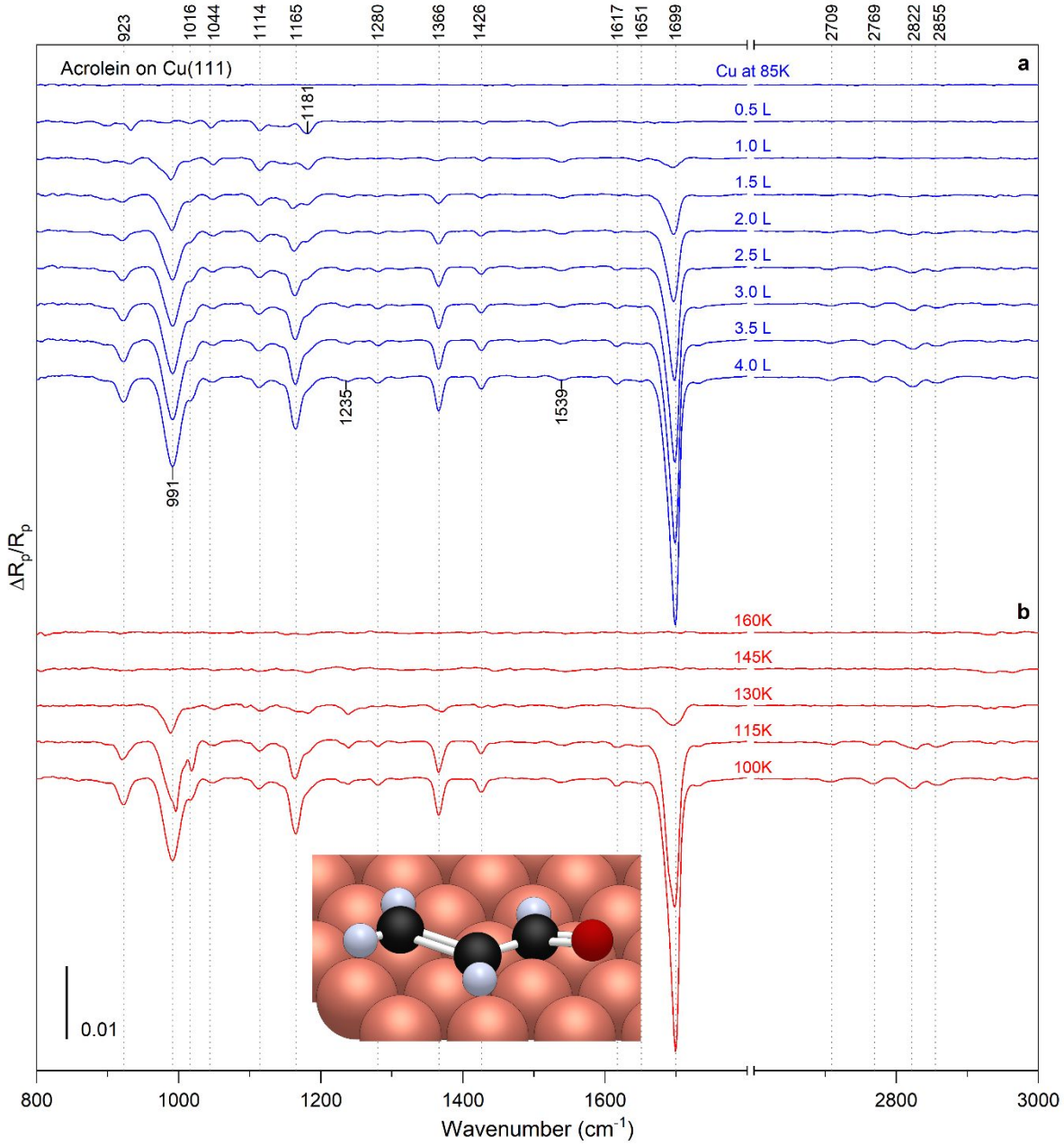

Fig. 1 a) RAIR spectra (blue) of acrolein on Cu(111) at 85 K versus exposures. b) RAIR spectra (red) after the Cu(111) surface at 85 K was exposed to 4 L of acrolein, annealed to the indicated temperatures for 1 minute, then cooled back to 85 K where the spectra were acquired. The inset shows the structure of monolayer acrolein on Cu(111).

Table 1 Comparison of vibrational assignments for acrolein multilayers on Au, Ag, and Pd surfaces. The f and v subscripts refer to formyl and vinyl, respectively.

Mode	Trans-acrolein Gas Phase[26]	Ag(111)[23]	Ag film[17]	Au(111)[14]	Pd(111)[13]	Cu(111)[a]	Ru(001)[27]
$\rho(CH_2)$	912	---	---	918,933	~915	923	920
$\omega(CH_2)$	959	978, 991	978, 991	964, 991	990	991	987
$\gamma(CH)_f$	972	1007	1007	1009	--	1016	--
$\gamma(CH)_v$	993	1019	1020	1020	--	1044	--
υ(C-C)	1158	1161	~1160	1159	1164	1165, 1181	1180
$\delta(CH)_v$				1281	1281	1280	1275
$\delta(CH)_f$	1360	1365	~1360	1365	1365	1366	1346
$\delta(CH_2)$	1420	1429	~1430	1425	1425	1426	1425
υ(C=C)	1625	1612	~1610	1614	1618	1617	1631
υ(C=O)	1724	1676	1674	1672, 1686	1650	1651	--
υ(C=O)	--	1687, 1696	1687,1697	1703	1699	1699	1989
$\upsilon(CH)_f$	3069	2704	n/a	n/a	2705	2709	2697
$2\delta(CH)_v$	--	2774	n/a	n/a	2766	2769	2760
$\upsilon_s(CH_2)$	2998	2823	n/a	n/a	2820	2822	2806
$\upsilon_a(CH_2)$	3103	2864	n/a	n/a	2857	2855	--

[a]This study

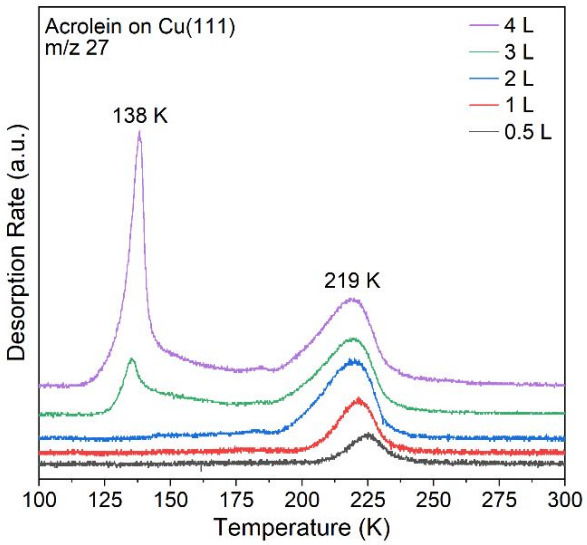

Fig. 2 TPD spectra of acrolein adsorbed on Cu(111) with increasing exposure.

3.2 Propanal

Fig. 3a shows RAIR spectra of propanal versus exposure after adsorption on Cu(111) at 85 K. Table 2 compares the peaks observed here and their assignments with those of gas and solid phase propanal and propanal on Ag(111), Pd(111) and Ru(001). At 0.5 L, the prominent peaks are assigned to CH_3 rocking modes (858, 898, and 1095 cm^{-1}), the CH_3 asymmetric bend (1458 cm^{-1}), the C=O stretch (both 1671 and 1735 cm^{-1}), and the CH_2 symmetric stretch (2961 cm^{-1}). At 1.0 L, a peak at 1382 cm^{-1} appears, which is midway between peaks in solid propanal at 1394 cm^{-1} assigned to the CH_3 symmetric deformation and 1374 cm^{-1} assigned to the CH bend.[28] A peak at 1683 cm^{-1} is resolved at 1.0 L and continues to grow and shifts to 1692 cm^{-1} at high exposures. A shoulder to the 1382 cm^{-1} peak at 1393 cm^{-1} appears and becomes prominent at 4.0 L. In the polycrystalline and liquid phases of propanal, two closely spaced C=O stretch peaks are also observed and are attributed to a Fermi resonance between the C=O stretch and the first overtone of the CCC symmetric stretch[28] or the first overtone of the CH_3 rock.[29] The 1735 cm^{-1} peak increases in intensity with exposure and is the most intense in the spectra for exposures of 1.0 L and above, which is a characteristic of solid propanal.[28] There is a pronounced change in the CH stretch region as the propanal exposure is increased

from 1.0 to 4.0 L. Initially, a peak at 2961 cm^{-1} is seen, but for higher exposures, two more peaks at lower and higher wavenumbers appear that grow in intensity. At 1.5 L, the 2961 cm^{-1} peak is no longer visible. Instead, the main peaks are at 2943 and 2980 cm^{-1}, and a new weaker peak at 2907 cm^{-1} becomes apparent. These four C-H stretch peaks are assigned to $\nu_s(CH_2)$ (2961 cm^{-1}), $\nu_s(CH_3)$ (2884 cm^{-1}), $\nu_{as}(CH_2)$ (2943 cm^{-1}), and $\nu_{as}(CH_3)$ (2980 cm^{-1}). The formyl C-H stretch is not observed. Two other peaks at 1343 and 1417 cm^{-1}, assigned to CH_2 wag and CH_3 symmetric deformation, continue to grow with increasing exposure.

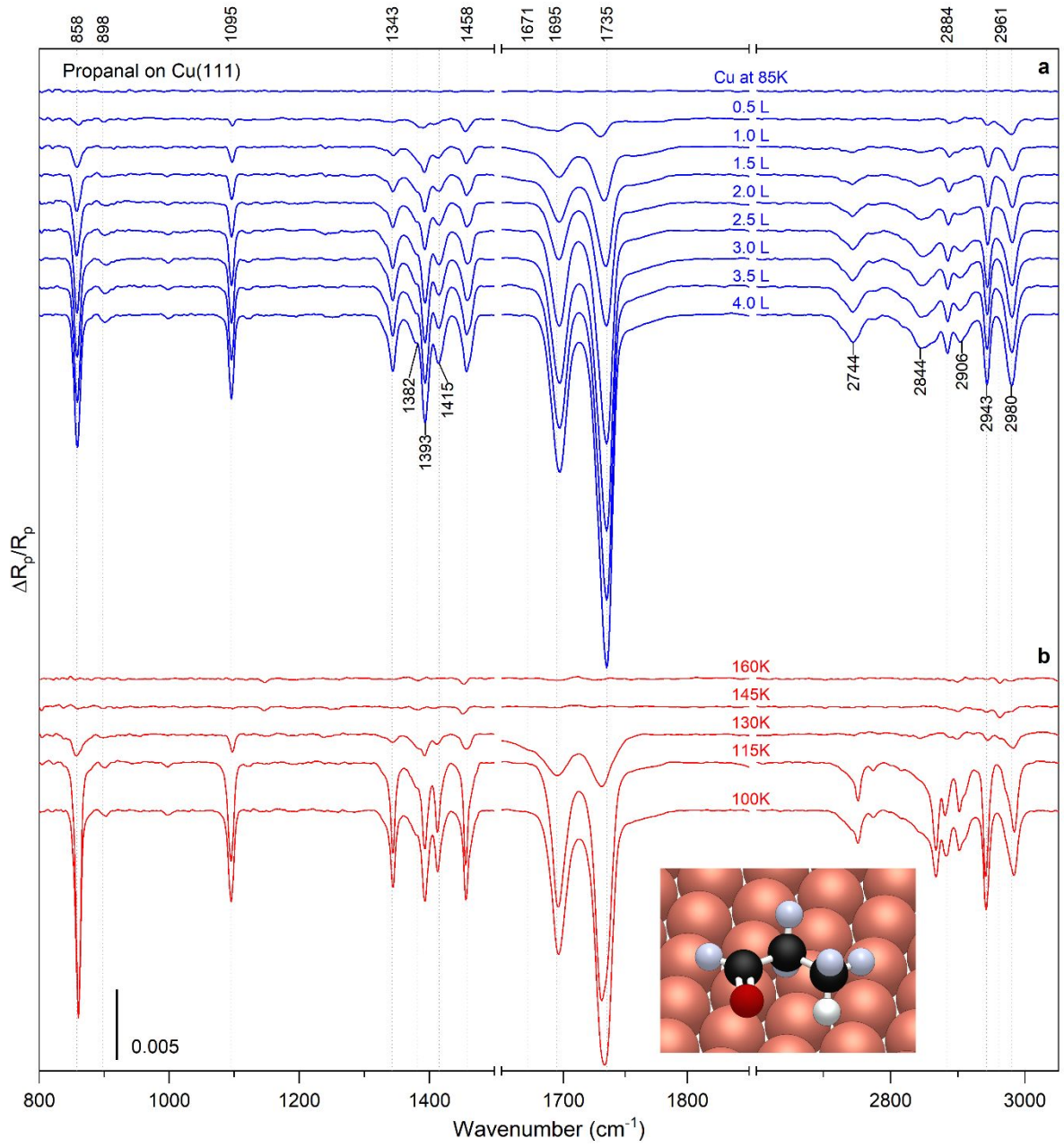

Fig. 3 a) RAIR spectra (blue) of propanal on Cu(111) at 85 K versus exposures. b) RAIR spectra (red) after the Cu(111) surface at 85 K was exposed to 4 L of propanal, annealed to the indicated temperatures for 1 minute, then cooled back to 85 K where the spectra were acquired. The inset shows the structure of monolayer propanal on Cu(111).

The TPD results for propanal on Cu(111) are shown in Fig. 4. A desorption peak at 150 K is observed for the monolayer, considerably lower than seen for acrolein in Fig. 2. Above 3.0 L, there is only a single multilayer desorption peak at 121 K, compared to the peak at 138 K in Fig. 2 for 2nd layer acrolein. Fig. 3b shows RAIR spectra following adsorption of 4.0 L of propanal at 85 K and annealing to the indicated temperatures. Only a modest change in the spectra after annealing up to 115 K suggests

that the structure adopted upon adsorption at 85 K is retained. After annealing to 130-145 K, the prominent peaks at 858, 1095, 1343, 1695, 1735, 2943, and 2980 disappeared, while the peak at 2961 cm^{-1} reappeared, which was observed in the unannealed spectrum at 0.5 L. The 130 K anneal desorbs the multilayer, which results in marked changes in the spectra. No peaks are observed after annealing to 160 K, indicating complete molecular desorption, consistent with the monolayer desorption temperature of 150 K seen in Fig. 4.

Table 2 Comparison of vibrational assignments for propanal

Vibrational Mode	Gas[28,30]	Solid[29]	Ag(111)[23]	Pd(111)[13]	Cu(111)[a]	Ru(001)[27]
$\rho(CH_3)$	--	860	--	--	858	--
$\rho(CH_3)$	892	897, 902	948	--	898	871
$\rho(CH_3)$	1098	1095	1095	1095	1095	1095, 1076
$\tau(CH_2)$	1250	1260	1248	--	--	--
$\omega(CH_2)$	1338	1368,1370	1347	1358	1343	1342
$\delta(CH)$	1364	1378	1387	1370	1382	1364
$\delta(CH_3)$	1409	1411,1414	1418	1413	1417	1389
$\delta_a(CH_2)$	1455	1465,1472	1460	1455	1458	1455
$2\rho(CH_3)$ FR $\upsilon(C=O)$	1693	1695	1686	1663, 1695	1671, 1695	1688
$\upsilon(C=O)$ FR $2\rho(CH_3)$	1754	1730	1730	1728	1735,1760	1630, 1658
$\upsilon(CH)$	2812	2863,2868	--	2868	--	--
$\upsilon_s(CH_3)$	2906	2877,2879	2884	2884	2884	2885
$\upsilon_a(CH_2)$	2906	2939	2944	2943	2943	2943
$\upsilon_s(CH_2)$	2954	2966,2968	2960	2904	2961	--
$\upsilon_a(CH_3)$	2981, 2992	2981,2982	2983	2960,2987	2980	2979

[a]This study

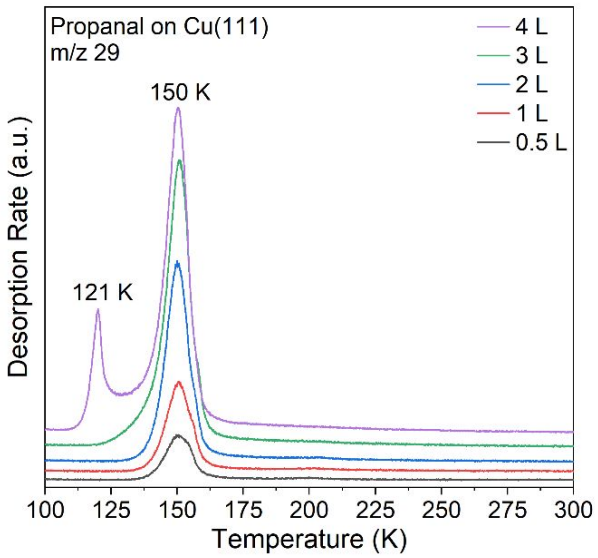

Fig. 4 TPD spectra of propanal adsorbed on Cu(111) at 85 K with increasing exposure.

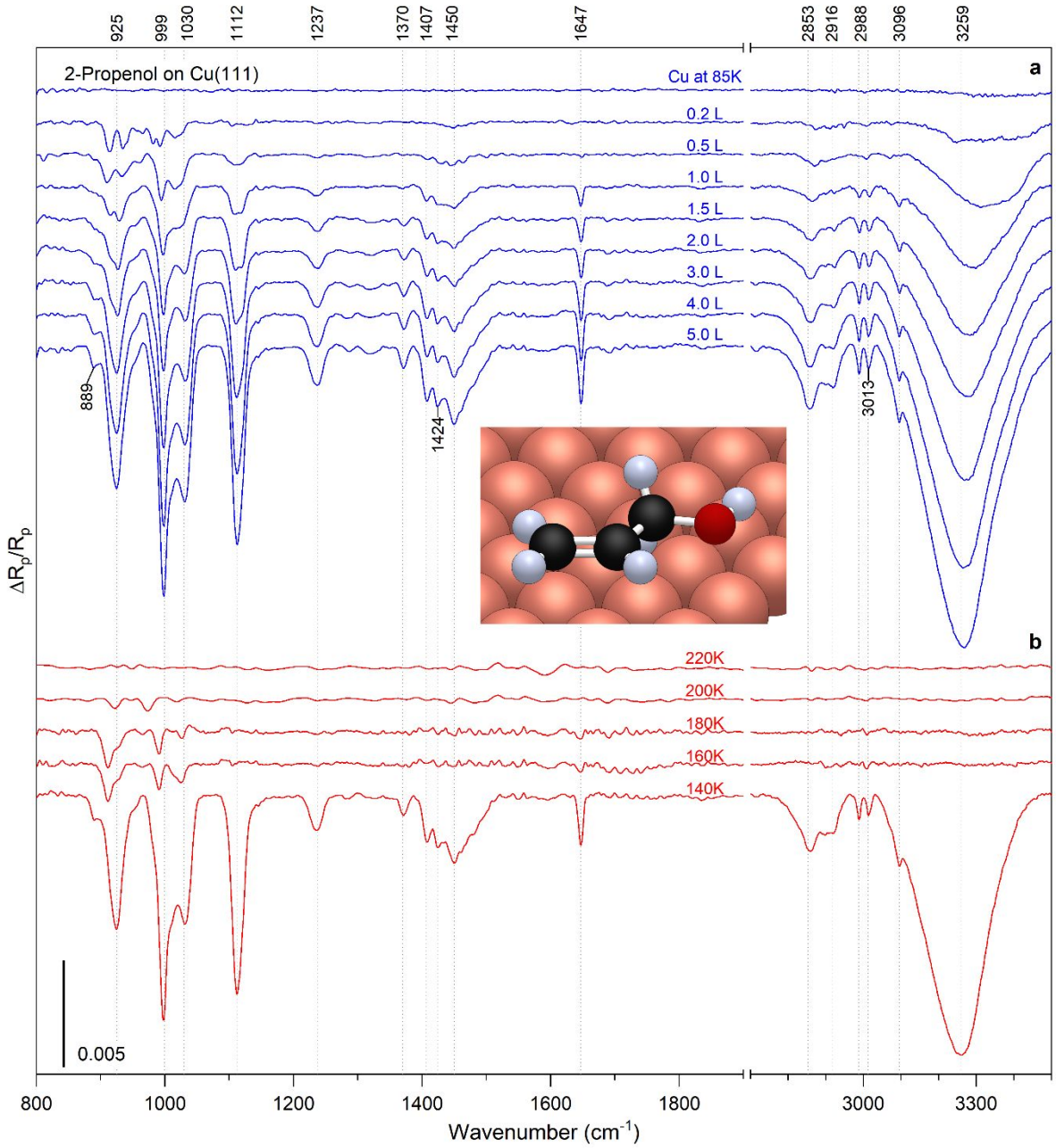

Fig 5. a) RAIR spectra (blue) of 2-propenol on Cu(111) at 85 K versus exposures. b) RAIR spectra (red) after the Cu(111) surface at 85 K was exposed to 5 L of propenol, annealed to the indicated temperatures for 1 minute, then cooled back to 85 K where the spectra were acquired. The inset shows the structure of monolayer 2-propenol on Cu(111).

3.3 2-Propenol

Fig. 5a shows RAIR spectra versus 2-propenol exposure to the Cu(111) surface at 85 K. For low exposures, there are four prominent peaks at 889, 925, 999, and 1030 cm^{-1}, which are assigned to the $=CH_2$ in-plane twist, the $=CH_2$ rock, $=CH_2$ wag, and the C-O stretch. With increasing exposure from 0.5 to 1.0 L, the 889 cm^{-1} peak becomes less intense while the 925, 999, and 1030 cm^{-1} peaks increase in intensity. For multilayer coverages at 1.0 L exposures, the bending modes of the $=CH_2$, C-H, and O-H groups and the stretching modes of the C=C, CH_2, and CH groups become visible. As the exposure increases to 5.0 L, these peaks all increase in intensity. Table 3 presents a complete assignment of the vibrational modes along with the reported frequencies of the most stable conformers of gas phase 2-propenol. Although the broadness of the peaks may have masked peaks of the other conformers, the values of the C-C and C-O stretch for the Gg conformer of gas phase 2-propenol most closely match those of 2-

propenol on the Cu(111) surface. In addition, During et al. reported fundamental frequencies for solid 2-propenol obtained by condensing the gas onto a CsI window at 77 K and included those frequencies in their table for the Gg conformer.[31] Our multilayer frequencies match those of the solid 2-propenol within a few cm^{-1}. The broad O-H stretch at 3264 cm^{-1}, strongly redshifted from its gas phase value of 3656 cm^{-1}, indicates hydrogen bonding between the 2-propenol molecules, even at the lowest exposure of 0.5 L. The C=C stretch at 1647 cm^{-1} appears only after a 1.0 L exposure suggesting that the C=C bond is parallel to the surface for the monolayer. Since the C=C stretch is not visible for the monolayer, the extent to which it is shifted through interaction with the Cu(111) surface is unknown.

Table 3 Comparison of vibrational assignments for 2-propenol. The gas phase values are for the different rotational conformers

Vibrational Mode	Gas Phase (Gg)[31]	Gas Phase (Cg)[31]	Gas Phase (Ct)[31]	Solid[31]	Ag(111)[23]	Pd(111)[13]	Cu(111)[a]	Ru(001)[27]
$\tau(=CH_2)$	908	919	--	--	--	~910	890	--
$\rho(=CH_2)$	938	--	--	919	925	--	925	929
$\rho(CH_2)$	918	966	--	--	979	--	--	--
$\omega(=CH_2)$	994	1000	982	994	992	1000, ~995	999	997
υ(-C-O-)	1038	1103	1131	1029	1033	~1030	1030	1022
υ(-C-C-)	1115	--	--	1112	1113	1113	1112	1119
$\tau(CH_2)$	1202	1191	--	--	--	--	--	--
δ(CH)	1286	--	--	1234	1231	1235	1237	1238
$\omega(CH_2)$	1320	1383	1436	--	--	--	--	--
δ(OH)	1371	1332	1206	1365	1368	1373	1370	1286
$\delta(=CH_2)$	1427	1412	1390	--	1407	1406	1407	--
				1421	1422	1424	1424	--
				1449	1449	1450	1450	1456
$\delta(CH_2)$	1461	1472	--	--	--	--	--	--
υ(C=C)	1655	1647	--	1649	1647	1648	1647	1647
$\upsilon_s(CH_2)$	2875	2883	--	2850	2857	2850	2853	2861
$\upsilon_a(CH_2)$	2933	--	--	2919	2917	2920	2916	2922
$\upsilon_s(=CH_2)$	2990	3031	3034	2990	2987	2989	2988	2987
υ(=CH)	3022	2999	--	3015	3015	3013	3013	3012
$\upsilon_a(=CH_2)$	3093	3102	3118	3090	3095	3092	3096	3098
υ(OH)	3656	3650	3689	--	3259	3260	3259	3323

[a]This study

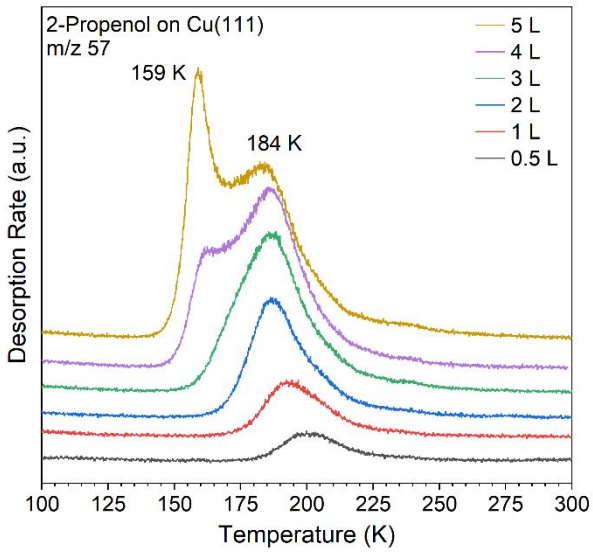

Fig. 6 TPD spectra of 2-propenol adsorbed on Cu(111) at 85 K with increasing exposure.

The TPD results in Figure 6 reveal that the 2-propenol monolayer desorbs beginning at 200 K, shifting to 184 K at higher exposures. The multilayer peak first appears as a shoulder for the 4 L exposure and develops into a distinct peak at 159 K for a 5 L exposure. The higher multilayer desorption temperature for 2-propenol compared with acrolein and propanal is attributed to stronger intermolecular interactions due to hydrogen bonding. On Ag(111), similar TPD results were obtained with the monolayer peak first appearing at 205 K and shifting to 202 K with increasing 2-propenol exposure, and a distinct multilayer desorption peak appearing at 176 K.

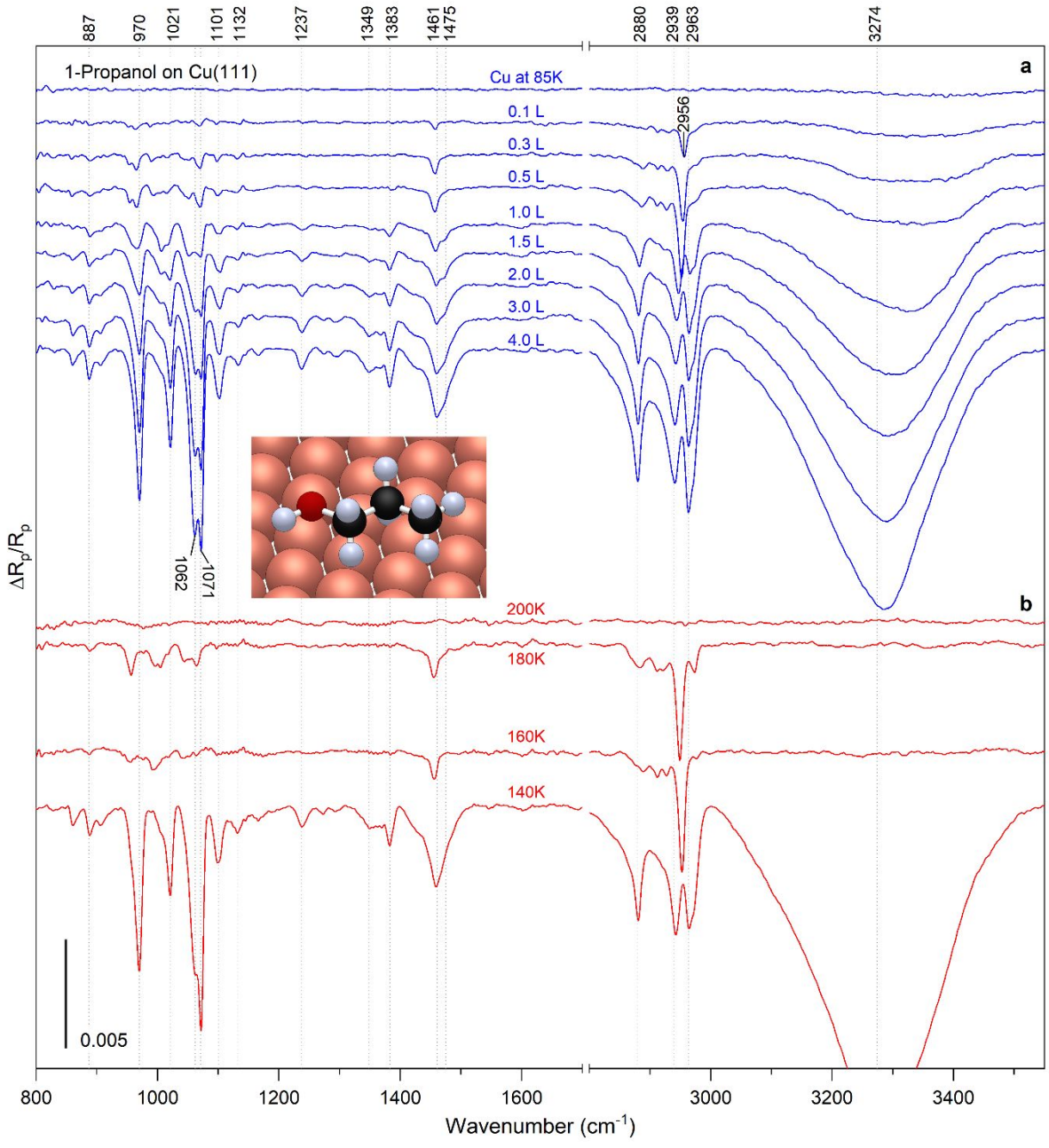

Fig. 7 a) RAIR spectra (blue) of 1-propanol on Cu(111) at 85 K versus exposures. b) RAIR spectra (red) after the Cu(111) surface at 85 K was exposed to 4 L of propanol, annealed to the indicated temperatures for 1 minute, then cooled back to 85 K where the spectra were acquired. The inset shows the structure of monolayer 1-propanol on Cu(111).

The results of annealing the Cu(111) surface after it had been exposed to 4.0 L of 2-propenol at 85 K are shown in Fig. 5b. Consistent with the TPD results in Fig. 6, annealing to 140 K leaves the multilayer on the surface and has little effect on the

spectrum. However, the 160 K anneal desorbs the multilayer leaving only molecules bound to the surface and causing several distinct changes; most prominently, the C=C stretch at 1647 cm^{-1} and the hydrogen-bonded OH stretch disappear. The loss of these peaks suggests that monolayer 2-propenol adsorbs with the O-H and C=C bonds parallel to the surface. The sharper peaks after annealing compared to the low coverage spectra after adsorption at 85 K may be due to greater structural order in the monolayer. Further annealing to 220 K should lead to complete desorption so that the remaining features between 925-1050 cm^{-1} in the 200 K spectrum are due to residual monolayer 2-propenol. If the 2-propenol interacts with the surface by π-bonding via the C=C bond, then the H_2C=CH– unit should be parallel to the surface and the out of plane CH_2 twist and wagging modes around 925 and 999 cm^{-1} would be expected to be most intense, as observed. Also, after the 160 K anneal, the C-O stretch at 1033 cm^{-1} is still visible and the C-O bond in the Gg conformer would be tilted away from the surface if the H_2C=CH– lies flat on the surface.

3.4 1-Propanol

Fig. 7a shows the RAIR spectra versus exposure of 1-propanol to the Cu(111) surface at 85 K. At the lowest exposure of 0.1 L, the IR bands seen at 1461 and 2956 cm^{-1} correspond to the CH_2 scissor and the CH_2 asymmetric stretch modes, respectively. With increasing exposure, the initially weak peaks in the CH stretch region at 2880, 2939, and 2963 cm^{-1} become more prominent and are assigned to the symmetric and asymmetric CH_2 stretches and the asymmetric CH_3 stretch. In addition, new peaks at 1237, 1349, 1383, 1475, 1696, and 1782 cm^{-1} appear. Table 4 provides a complete assignment of the vibrational modes. In the low wavenumber range, the peaks at 970, 1021, and 1062 cm^{-1} also appear close to gas phase fundamentals at 971, 1013, and 1066 cm^{-1}. The modes in this range are a mix of CH_3 rock, and CCC stretch internal coordinates. For multilayer exposures, a shoulder at 1475 on the 1461 cm^{-1} peak appears and the intensity of all peaks increases with increasing exposures. In addition, a broad redshifted OH stretch is observed for all exposures, indicating hydrogen bonding between 1-propanol molecules. The peaks observed in this study are compared to previous studies of the gas phase and adsorbed 1-propanol on Ag(111)[23], Cu(111)[20], Rh(111)[21], and Ru(001)[27] surfaces in Table 4.

Table 4 Comparison of vibrational assignments for 1-propanol

Vibrational Mode	Gas Phase[32]	Ag(111)[23]	Cu(111)[20]	Rh(111)[21]	Cu(111)[a]	Ru(001)[27]
υ_a(C-C-O)	971	967	972	1040	970	971
υ_a(C-C-C)	1013	1018	1023	--	1021	1009
$\rho(CH_3) + \upsilon$(CC)	1066	1070, 1100	1103, 1074	1040	1062, 1071	1105, 1161
$\rho(CH_2)$	--	--	--	--	1101,1132	1136
δ(COH)	1218	1234	1239	--	1237	1228
$\tau(CH_2)$	--	--	1294	--	1349	1292
$\omega(CH_2)$	1393	1384	1365	1390	1383	1382
$\delta(CH_2)$ -scissor	1464	1456	1475	1495	1461, 1475	1458
$\upsilon_s(CH_2)$	2892	2877	2877	--	2880	2881
$\upsilon_a(CH_2)$	--	2943	2937	--	2939	2942
$\upsilon_a(CH_3)$	2978	2960	2965	2970	2963	2966
υ(OH)	3687	3273	3275	3205	3274	3280

[a]This study

Fig. 8 shows the TPD results versus 1-propanol exposure to Cu(111) at 85 K. The 155 K peak corresponds to 1-propanol multilayers, while the peak at 196 K corresponds to the desorption of the monolayer. Similar but not identical results were observed on Ag(111) with the multilayer desorbing in the range of 178-184 K and the monolayer peak increasing from 211 to 219 K with increasing coverage. This comparison indicates slightly higher binding energies for 1-propanol on Ag(111) than on Cu(111). The difference in the monolayer binding has a slight influence on the multilayer desorption despite the expectation that only interactions between molecules determine the multilayer desorption temperature. On both surfaces, the alcohols 2-propenol and 1-propanol show higher desorption temperatures compared to the molecules without OH bonds, acrolein, and propanal. Evidently, the ability of the molecules to form intermolecular hydrogen bonds is a significant factor stabilizing their adsorption on metal surfaces.

Fig. 7b shows RAIR spectra after adsorbing 4.0 L of 1-propanol on the Cu(111) surface at 85 K and after annealing to the indicated temperatures. For annealing temperatures of 140 K and below, no changes are observed. However, pronounced differences are seen for the 160 K anneal, which should desorb the multilayer according to the TPD results in Fig. 8. No hydrogen bonding was observed in the monolayer, as indicated by the absence of the O-H stretch, as was the case for 2-propenol. The 160 and 180 K spectra show several sharp peaks, most prominently at 1461 and 2950 cm^{-1}. Although similar results were obtained on

Ag(111), in that case the peaks after annealing to 160 K were considerably sharper. For example, by using an experimental resolution of 1 cm^{-1}, the intrinsic full width at half maximum (FWHM) of the 2948 cm^{-1} peak on Ag(111) was calculated to be 4.0 cm^{-1}. Using 2 cm^{-1} resolution, we determined that the intrinsic FWHM of the corresponding peak on Cu(111), which occurs at 2954 cm^{-1} after the 180 K anneal, is 10.4 cm^{-1}. Furthermore, other peaks of 1-propanol on Ag(111) are even sharper, with FWHM of 1.6 and 1.1 cm^{-1} for the $\delta(CH_2)$-scissor mode at 1455 cm^{-1} and the υ_a(C-C-C) mode at 1015 cm^{-1}, respectively. On the Ag(111) surface, we attributed the simplicity of the spectrum consisting of just a few extremely sharp peaks to the presence of only one of the five possible conformers of 1-propanol on the surface.[33] While the 160 and 180 K anneals have a somewhat similar effect on the spectra for 1-propanol on Cu(111), the evidence for the presence of only one conformer is not as compelling due to the greater number of peaks, particularly in the region below 1100 cm^{-1}, and their higher FWHM. The 180 K spectrum in Fig. 7b is also similar to the unannealed spectrum of 0.5 L of 1-propanol (Fig. 7a), suggesting that in both cases the spectra are characteristic of the monolayer. All IR features are lost after further annealing to 200 K, which is consistent with the TPD results showing that the monolayer is completely desorbed by this temperature. The absence of any peaks after the 200 K anneal is consistent with the lack of reaction to produce any new species, such as 1-propoxide, which forms from the reaction of 1-propanol with adsorbed oxygen on the Cu(111) surface.[20]

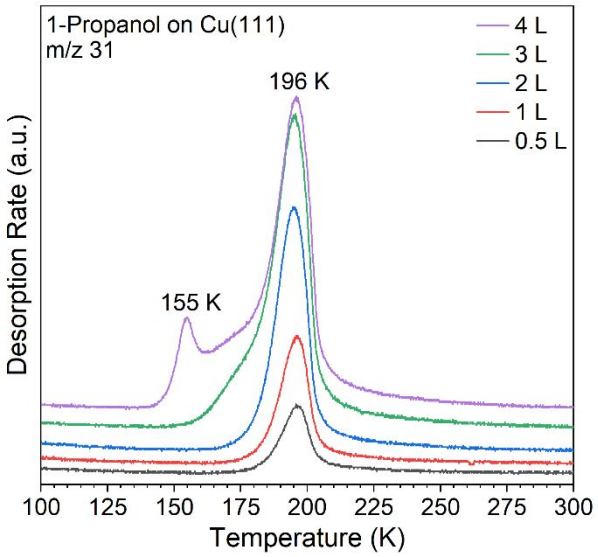

Fig. 8 TPD spectra of 1-propanol on Cu(111) adsorbed at 85 K with increasing exposure.

4. Conclusions

Acrolein and its three hydrogenation products, propanal, 2-propenol, and 1-propanol all desorb from the Cu(111) surface in distinct multilayer and higher temperature monolayer peaks indicating that while the bonding to the metal surface for the monolayer molecules is weak, it is stronger than the intermolecular interactions between molecules in the multilayer. The RAIR spectra for the multilayer are very similar to those of the molecular solids. In light of the surface selection rules, this indicates that the molecules are randomly oriented in the multilayers. In contrast, when observed, the spectra of the monolayer molecules feature fewer peaks, suggesting a definite orientation with respect to the surface normal. For the planar acrolein molecule, the lack of any observable RAIRS peaks for the monolayer is consistent with the molecular plane oriented parallel to the surface. For the two alcohols, 2-propenol and 1-proponal, the strongly redshifted OH stretch of the multilayers is absent for the monolayers indicating that the hydrogen bonding in the multilayers is absent for the monolayer. Comparison to a similar study of these molecules on the Ag(111) surface reveals differences in both the RAIR spectra and the binding energies as reflected in differences in the monolayer desorption temperatures. For example, monolayer acrolein desorbs more than 50 K higher from Cu(111) than from Ag(111). The higher desorption temperature from Cu(111) makes it more likely that acrolein could undergo hydrogenation before desorption if H atoms were supplied either from adsorption of atomic hydrogen or from spill-over from an active metal in a single atom alloy.

Author Contributions

AI obtained the RAIRS spectra, prepared the final figures, and wrote the first draft of the manuscript. DLM obtained the TPD results and prepared the initial TPD figures. MT assisted with data interpretation and revisions to the manuscript.

Conflicts of interest

There are no conflicts to declare.

Acknowledgments

This work was supported by a grant from the National Science Foundation, CHE-2102622.

References

1. M. Luneau, J. S. Lim, D. A. Patel, E. C. H. Sykes, C. M. Friend and P. Sautet, *Chem. Rev.*, 2020, **120**, 12834-12872.
2. P. Claus, *Top. Catal.*, 1998, **5**, 51-62.
3. K. A. D. Swift, *Top. Catal.*, 2004, **27**, 143-155.
4. W. Schwab, R. Davidovich-Rikanati and E. Lewinsohn, *Plant J.*, 2008, **54**, 712-732.
5. F. Delbecq and P. Sautet, *J. Catal.*, 1995, **152**, 217-236.
6. F. Delbecq and P. Sautet, *J. Catal.*, 2002, **211**, 398-406.
7. T. B. L. W. Marinelli, S. Nabuurs and V. Ponec, *J. Catal.*, 1995, **151**, 431-438.
8. R. T. Hannagan, G. Giannakakis, M. Flytzani-Stephanopoulos and E. C. H. Sykes, *Chem. Rev.*, 2020, **120**, 12044-12088.
9. M. Muir, D. L. Molina, A. Islam, M. K. Abdel-Rahman and M. Trenary, *J. Phys. Chem. C*, 2020, **124**, 24271-24278.
10. C. R. O'Connor, K. Duanmu, D. A. Patel, E. Muramoto, M. A. van Spronsen, D. Stacchiola, E. C. H. Sykes, P. Sautet, R. J. Madix and C. M. Friend, *Proc. Natl. Acad. Sci. U. S. A.*, 2020, **117**, 22657-22664.
11. A. E. Baber, H. L. Tierney, T. J. Lawton and E. C. H. Sykes, *ChemCatChem*, 2011, **3**, 607-614.
12. G. Kyriakou, M. B. Boucher, A. D. Jewell, E. A. Lewis, T. J. Lawton, A. E. Baber, H. L. Tierney, M. Flytzani-Stephanopoulos and E. C. Sykes, *Science*, 2012, **335**, 1209-1212.
13. K. H. Dostert, C. P. O'Brien, F. Mirabella, F. Ivars-Barcelo and S. Schauermann, *Phys. Chem. Chem. Phys.*, 2016, **18**, 13960-13973.
14. M. Akita, N. Osaka and K. Itoh, *Surf. Sci.*, 1998, **405**, 172-181.
15. L. E. Murillo and J. G. Chen, *Surf. Sci.*, 2008, **602**, 919-931.
16. D. A. Esan, Y. Ren, X. Feng and M. Trenary, *J. Phys. Chem. C*, 2017, **121**, 4384-4392.
17. S. Fujii, N. Osaka, M. Akita and K. Itoh, *J. Phys. Chem.*, 1995, **99**, 6994-7001.
18. D. A. Esan and M. Trenary, *Top. Catal.*, 2018, **61**, 318-327.
19. K. H. Dostert, C. P. O'Brien, F. Ivars-Barcelo, S. Schauermann and H. J. Freund, *J. Am. Chem. Soc.*, 2015, **137**, 13496-13502.
20. S. C. Street and A. J. Gellman, *Surf. Sci.*, 1997, **372**, 223-238.
21. N. F. Brown and M. A. Barteau, *Langmuir*, 2002, **8**, 862-869.
22. J. Gong, T. Yan and C. B. Mullins, *Chem Commun*, 2009, 761.
23. M. Muir, D. L. Molina, A. Islam, M. K. Abdel-Rahman and M. Trenary, *Phys. Chem. Chem. Phys.*, 2020, **22**, 25011-25020.
24. J. D. Krooswyk, I. Waluyo and M. Trenary, *ACS Catal.*, 2015, **5**, 4725-4733.
25. A. Islam, M. K. Abdel-Rahman and M. Trenary, *J. Phys. Chem. C*, 2021, **125**, 18786-18791.
26. C. Puzzarini, E. Penocchio, M. Biczysko and V. Barone, *J. Phys. Chem. A*, 2014, **118**, 6648-6656.
27. D. A. Esan and M. Trenary, *Phys. Chem. Chem. Phys.*, 2017, **19**, 10870-10877.
28. G. A. Guirgis, B. R. Drew, T. K. Gounev and J. R. Durig, *Spectrochim. Acta, Part A*, 1998, **54**, 123-143.
29. G. Sbrana and V. Schettino, *J. Mol. Spectrosc.*, 1970, **33**, 100-+.
30. B. Köroğlu, Z. Loparo, J. Nath, R. E. Peale and S. S. Vasu, *J. Quant. Spectrosc. Radiat. Transfer*, 2015, **152**, 107-113.
31. J. R. Durig, A. Ganguly, A. M. E. Defrawy, C. Zheng, H. M. Badawi, W. A. Herrebout, B. J. v. d. Veken, G. A. Guirgis and T. K. Gounev, *J. Mol. Struct.*, 2009, **922**, 114-126.
32. K. Fukushima and B. J. Zwolinski, *J. Mol. Spectrosc.*, 1968, **26**, 368-383.
33. R. Ranjan, M. Muir, D. L. Molina and M. Trenary, *J. Phys. Chem. C*, 2022, **126**, 7281-7287.

